

Variation of microfibril angle, density and fibre orientation in twenty-nine *Eucalyptus nitens* trees

ROBERT EVANS*, SHAREE STRINGER† AND R. PAUL KIBBLEWHITE‡

SilviScan-2 was used to estimate and map microfibril angle (MFA) and density in twenty-nine 15-year-old *Eucalyptus nitens* trees. Over 4000 MFA measurements were made at about 100/hour. Each measurement represented a weighted average for about 50000 fibres. After an initial decrease near ground level, density increased with height in the stem. MFA decreased with height in the stem, reached a minimum around 30 to 50% of tree height, then increased towards the top. In the radial direction, density first decreased for a few years, then increased towards the bark. MFA was in the range 20 to 30 degrees near the pith at all heights and generally decreased towards the bark over most of the height of the stem. The lowest MFA values (approx. 10 degrees) were found close to the bark at 30 to 50% of stem height. Both density and MFA varied more rapidly near ground level, increasing the uncertainty of correlations between breast-height properties and whole tree properties. On some samples, high-resolution (0.2 mm) MFA scans were performed to confirm an earlier finding that MFA is strongly inversely correlated with density over a few growth rings but not over larger distances. X-ray diffraction was also used for estimating the orientation of the fibres within the samples. The radial variation in fibre orientation generally decreased with distance from the ground. Breast-height sample properties were moderate to good predictors of whole tree properties. Better correlations were

obtained using samples from 5.5 m. Whole tree average density and MFA were found to be uncorrelated, indicating that tree improvement strategies could be designed to simultaneously optimise these properties.

KEYWORDS

Microfibril angle, X-ray densitometry, X-ray diffractometry *Eucalyptus nitens*, distributions, whole tree maps

Determination of averages and distributions of properties of fibres in wood is a necessary first step in the search for relationships between wood fibre properties and pulp and paper properties. In previous reports, we presented the results of SilviScan analysis of a single *E. nitens* tree. We have since extended the study to twenty-nine trees sampled at five, six or seven heights, depending on tree height. These trees had already been intensively evaluated at Forest Research (Rotorua, NZ) for wood, pulp and paper properties (1). Radial strips from all sampled heights in the 29 trees were then examined using SilviScan-2 (2) at the Cooperative Research Centre for Hardwood Fibre and Paper Science. We present here some results of our initial investigation into the within- and between-tree variation of microfibril angle and density. Fibre orientation, measured during MFA analysis, is discussed briefly.

EXPERIMENTAL

Samples

Twenty-nine 15-year-old *E. nitens* trees of central Victorian provenances were selected for their wide range in density as determined

from 5 mm breast-height increment cores. The trees were grown in a provenance-progeny trial, planted in 1979 in Kaingaroa Forest, about 100 km southeast of Rotorua on New Zealand's North Island. Discs were taken from a range of heights within each tree (nominally 0, 1.4, 5.5, 11, 16.5, and 22 m where possible). The tallest trees were sampled also at a nominal 27.5 m.

Radial sections were cut from the green discs, dehydrated in ethanol, dried and stored for analysis at CSIRO Forest Products Laboratories. Sample strips for SilviScan-2 analysis were prepared from the dried radial sections using methods previously reported (2).

Densitometry

The densitometry measurements were made at a rate of 100 mm/min using the CCD detector system on SilviScan-2. The average density of each sample was determined gravimetrically and used to normalise each density profile. A typical series of images from the densitometer camera is shown as a composite image in Figure 1. Figure 2 is a composite X-ray image of a transverse section, in which the 2-D density variation is evident. Use of transverse sections would simplify determination of high-resolution density profiles, accounting for the presence of vessels and curved ring boundaries. However, such a configuration cannot be used for rapid MFA analysis because the most intense diffraction peak (002) cannot be analysed when the X-ray beam is approximately parallel to the fibre axis. Therefore, to avoid preparing matched pairs of orthogonal samples, both densitometric and diffractometric analyses

* Senior Principal Research Scientist

† Technical Officer, Cooperative Research Centre for Hardwood Fibre and Paper Science, CSIRO Forestry and Forest Products, Private Bag 10, Clayton South MDC, Victoria 3169, Australia.

‡ Senior Scientist, PAPRO New Zealand, Forest Research, Private Bag 3020, Rotorua, New Zealand.

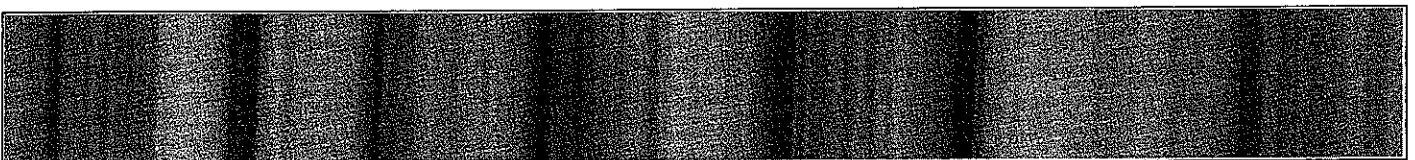


Fig. 1 Composite X-ray absorption image of a 35 mm long radial/longitudinal section of *E. nitens* obtained on the SilviScan-2 densitometry system. The X-ray beam direction is normal to the page (tangential direction). Darker greys correspond to greater X-ray absorbances and therefore higher wood densities. The fine structure is caused in part by vessels. The sloping grain seen in this sample is a common effect taken into account by the software in determining the density profile.

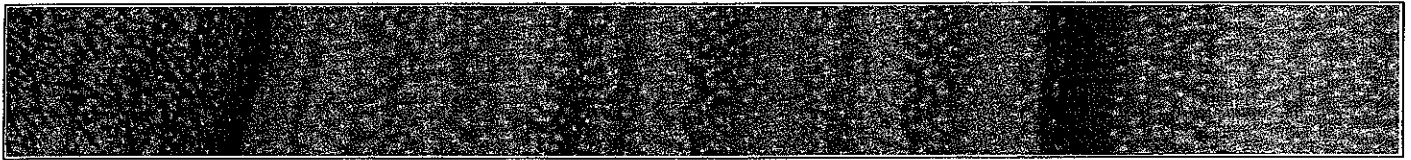


Fig. 2 Composite X-ray absorption image for a 3.5 mm long transverse section of *E. nitens* (different from the sample in Figure 1) recorded using the SilviScan-2 densitometry system. The X-ray beam is in the longitudinal direction (along the fibre axes, normal to the page). Although this configuration would be more suitable for high-resolution densitometry, it is not suitable for microfibril angle analysis using the 002 reflection.

on SilviScan-2 are done with the X-ray beam in the tangential direction. The densities reported in this paper are not corrected for the presence of vessels. SilviScan-2 image analysis of these samples, required for the determination of vessel-free density, was being carried out at the time of writing and will be presented in a future report.

Unless otherwise stated, the term 'density' refers to density after conditioning at 20°C and 40% RH from below.

Microfibril angle

MFA was estimated from the cellulose-1 002 azimuthal X-ray diffraction peaks obtained with a rapid scanning X-ray diffractometer system in integration mode (2). The integration length was 5 mm and the acquisition time per measurement was 30 seconds. All fibres in the sample cross-section contributed to the MFA averages (2).

Over 4000 individual MFA measurements were made. Although $\sim 10^8$ fibres contributed to the results, only 1 part in 10^6 of tree volume was analysed for density and 1 part in 10^7 for MFA.

Fibre orientation

MFA measurements on wood using the 002 reflection from cellulose-1 usually require the fibres to be perpendicular to the X-ray beam. If the fibre axes are tilted in the direction of the beam, the diffraction peaks broaden, leading to overestimation of MFA. If the fibre axes are rotated around the beam direction, the diffraction pattern simply rotates and no MFA correction is required. In our system, we measure the distortion to correct the MFA results for the effects of fibre tilt in the beam direction. The first advantage of this method is that we do not need to adjust the orientation of the sample for each measurement; the second advantage is that we obtain information on the 3-D orientation of the fibres at each measurement position. A description of the method will be presented in a future report.

RESULTS AND DISCUSSION

For one set of samples from one tree, the following outputs are obtained for each property:

Radial property profile

Growth ring
positions
widths
areas
volumes

Property

means
standard deviations
medians
10,25,75,90 percentiles

Distance-based and area-based tree maps of:

ring means
ring medians
standard deviations
percentile ranges

Distributions

within rings at each height
within samples at each height
within growth shells
within the whole tree

The information presented in this report represents a small cross-section of the data produced by SilviScan-2. A summary is given in the Appendix (Tables A1 and A2), together with basic densities obtained in earlier work (1).

Conditioned density and basic density

It has been found (3), using Chudnoff's data (4) on a very wide range of wood from 379 tropical trees, that basic density (D_b) can be predicted from conditioned density (D_c , 12% moisture content) using the relationship (thick line) shown in Figure 3.

Our data for 29 *E. nitens* varies over a much smaller range than the data in (4). Regression lines tend to tilt towards the x-axis (lower slope) as the range is reduced at constant standard error. We therefore forced the regression line for our data to have the same slope as that for Chudnoff's (3,4) data. This made no significant difference to the quality of the fit ($R^2 = 0.94$). Assuming no difference in the accuracy of the basic density data, our conditioned densities are approximately

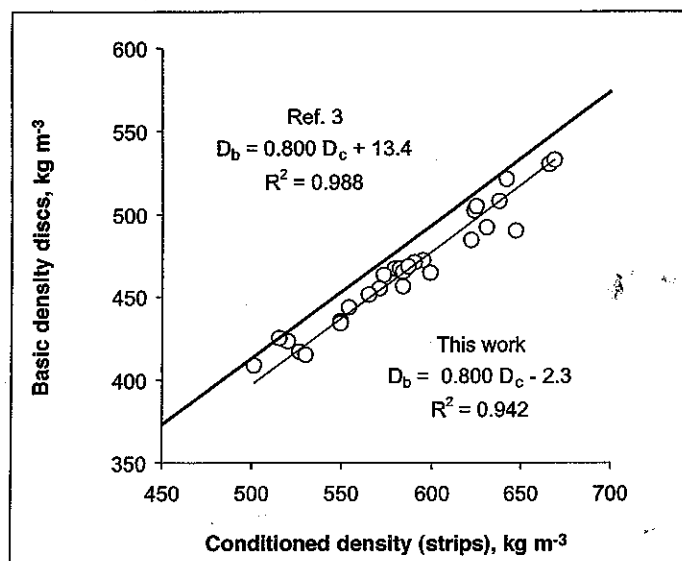


Fig. 3 Prediction of whole tree basic density of 29 *E. nitens* trees from whole-tree conditioned density interpolated from radial strip density profiles from SilviScan-2. Our regression line (thin) was forced to be parallel with a published (3) relationship (thick line) for 379 trees.

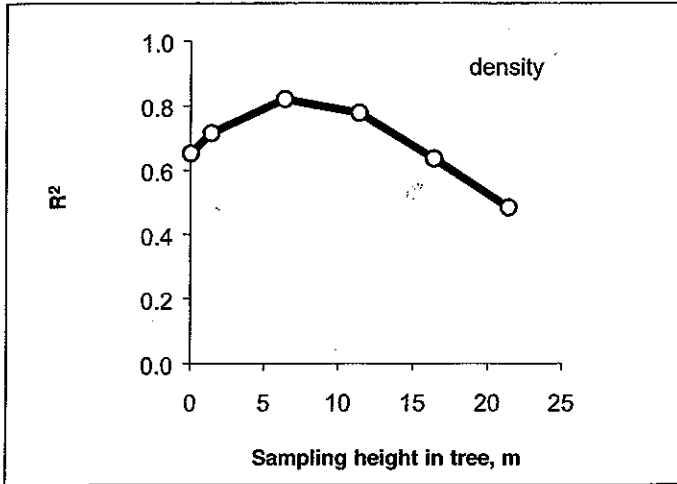


Fig. 4 Effect of sampling height on the prediction of whole tree density.

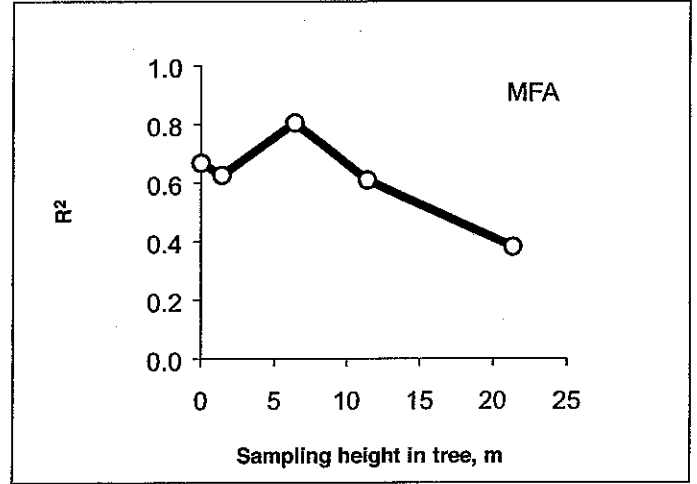


Fig. 5 Effect of sampling height on prediction of whole tree MFA.

3% higher than those found by Chudnoff (4). The low residual standard error in our data (8 kg m^{-3}) implies that cell collapse on drying was not a significant effect. We also saw no evidence of collapse in micrographs of the polished transverse sample surfaces. This is the principal reason ethanol was chosen to dehydrate our samples.

Sampling for whole-tree density and MFA

Figures 4 and 5 show the effect of sampling position on the prediction of whole-tree density and MFA. The best sampling height was 5.5 m. As non-destructive sampling is impractical at this height, it is more cost-effective to sample a larger number of trees at BH to recover some of the lost precision. If individual trees need not be preserved, samples could be taken from ~5 m to give more accurate results, especially if whole diameters are used (2).

Distributions

The frequency distributions of conditioned density and MFA were calculated from the volume-weighted profiles obtained from SilviScan-2. Average distributions for all 29 trees are shown in Figures 6 and 7. These distributions do not include the local variation within the measurement zones. Distributions based on single fibre measurements would be broader than the ones shown here.

Figures 8 and 9 show the extreme frequency distributions for these trees. Tables A1 and A2 in the Appendix include a summary (in terms of percentiles and means) of the MFA and density distributions for all trees.

Effect of tree age

In an earlier study of a single 18-year-old *E. nitens* tree (2) we found that whole tree average MFA decreased from about 25 degrees to about 17 degrees between 6 and 18 years, while whole-tree average density remained almost constant.

The results presented here for 29 15-year-old *E. nitens* trees show that whole-tree average MFA decreased from about 19 degrees at age 3 to about 14 degrees at age 15. Whole-tree average density increased from 470 kg m^{-3} to 580 kg m^{-3} . Variation between trees was very large for both density and MFA (Fig. 10 and 11). The trend lines for the 29 trees tend to be approximately parallel, indicating a significant age-age correlation. The average trends are shown in Figures 12 and 13.

Early age selection

The information presented graphically in Figures 10 and 11 can be used to investigate the accuracy of early age selection. For example, the 29 trees may be ranked in increasing order of density at any age, and those trees with density above the median value (14 trees out of 29) chosen for breeding. For these trees, we know the density at all ages; therefore it is possible

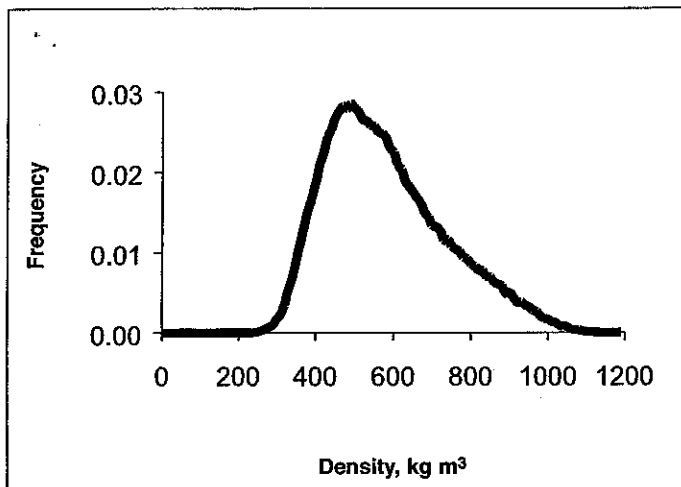


Fig. 6 Average density whole-tree density distribution for 29 trees.

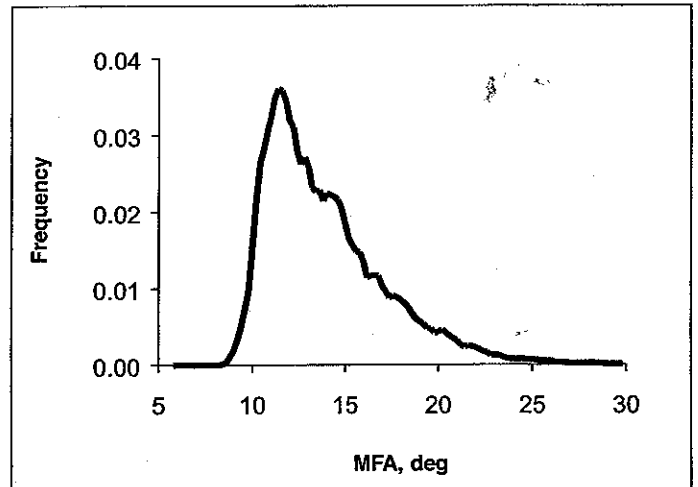


Fig. 7 Average whole tree MFA distribution for 29 *E. nitens* trees.

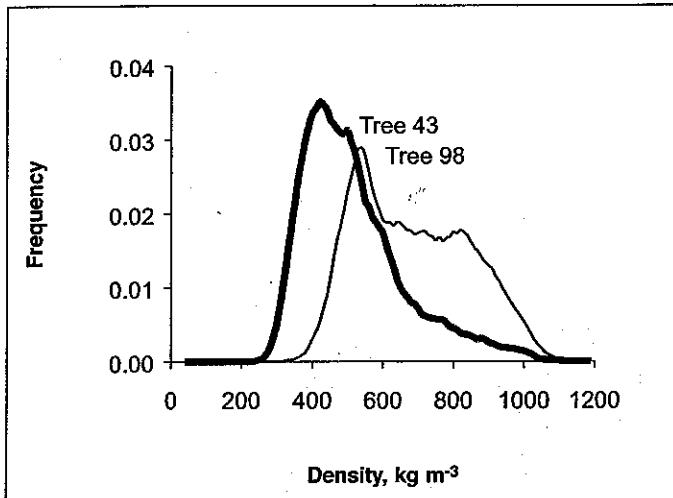


Fig. 8 Extreme whole-tree density distributions for individual *E. nitens* trees.

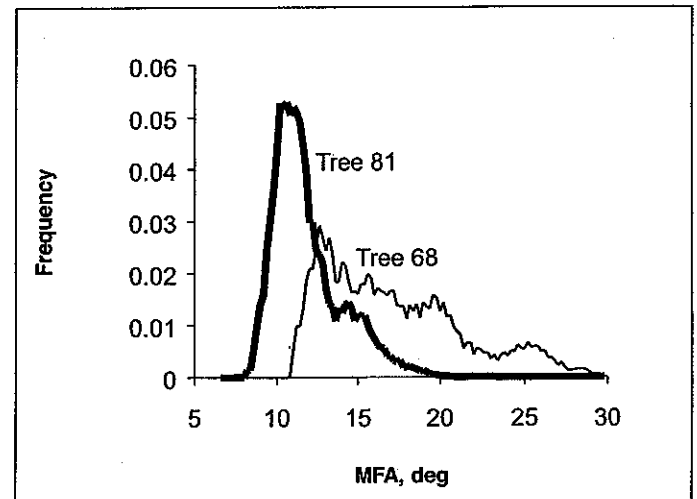


Fig. 9 Extreme whole-tree MFA distributions for individual *E. nitens* trees.

to determine how many trees would be misclassified at any subsequent age (15 years in this case). Table 1 shows the results of attempts to predict the 14 trees that would have the highest density or the lowest MFA at age 15.

For example, the trees may be ranked on MFA at age 6 and the 14 trees with MFA below the median value chosen. Had the trees continued to grow until age 15, three low MFA trees would have been missed.

Whole-tree maps

Whole-tree maps of density and MFA were produced by interpolation of the radial profile data between sampling heights. The 29 maps for each property

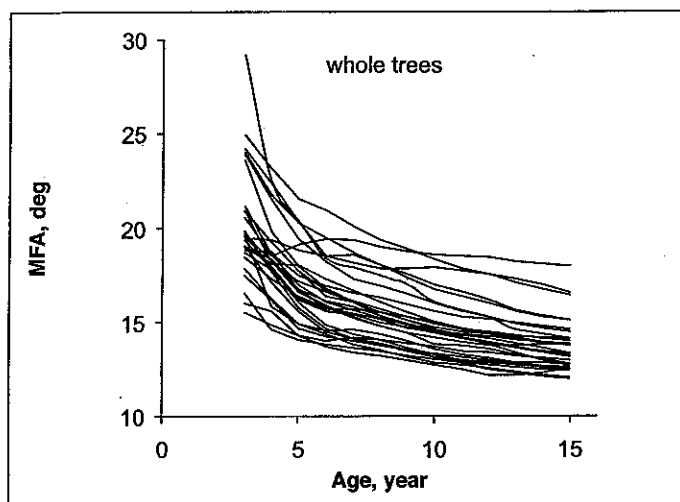


Fig. 10 Effect of age on whole-tree average MFA for each of the 29 *E. nitens* trees.

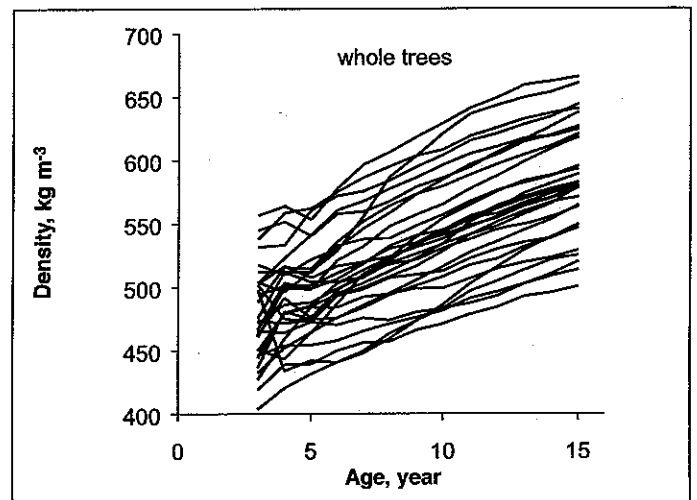


Fig. 11 Effect of age on whole-tree average density for each of the 29 *E. nitens* trees.

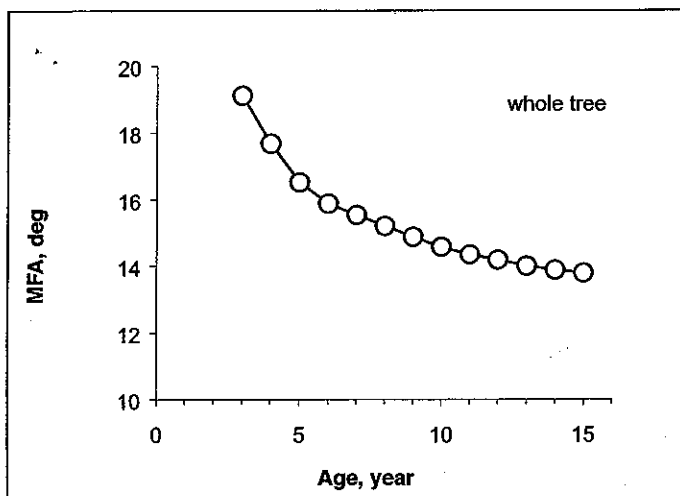


Fig. 12 Whole-tree average MFA vs. age for 29 *E. nitens* trees.

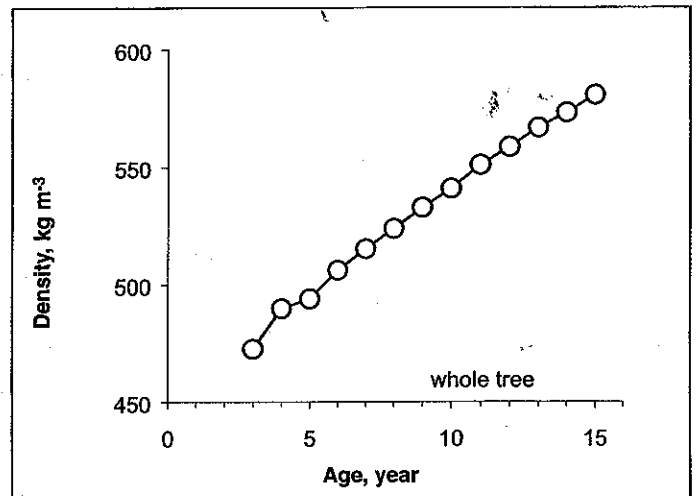


Fig. 13 Whole-tree average density vs. age for 29 *E. nitens* trees.

Table 1

Selection of trees with average MFA below the median or with average densities above the median at age 15. Trees missed out of 14 at each selection age.

Age at selection years	Low MFA trees missed out of 14	High density trees missed out of 14
15	0	0
14	0	0
13	0	0
12	1	0
11	1	1
10	2	1
9	2	2
8	2	2
7	2	2
6	3	3
5	3	3
4	4	3
3	4	5
2	5	6

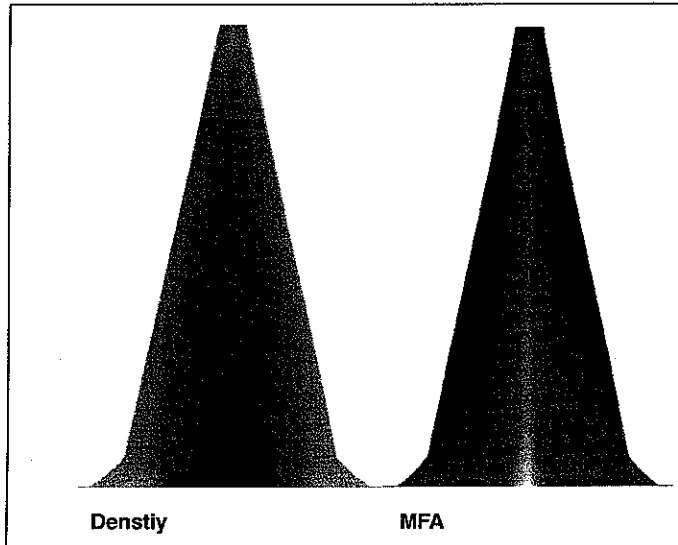


Fig. 14 Average whole-tree maps of density and microfibril angle. Lighter shades indicate higher values. These images are based on an area scale. Areas represent volumes in the tree.

were fitted to the average tree form and averaged to produce the images shown in Figure 14. Areas in these maps represent volumes in the tree; distance from the pith at any height in the tree corresponds to area of wood produced at that height. The patterns of variation are discussed below in more detail.

High-resolution density and MFA profiles.

In general, MFA decreased from pith to bark, but near ground level MFA often decreased initially then increased towards the bark. Figures 15 and 16 show the MFA and density profiles for samples taken at the base of tree 68 and at the 5.5 m level of tree 43.

The multiple relationships shown in Figure 17 were obtained from sections of the data in Figure 15, and show that there is no single global correlation between MFA and density. We have observed that fibre wall thickness is the main determinant of wood density in *E. nitens* and *E. globulus*. Following Hiller's arguments (5), thicker cell walls have a

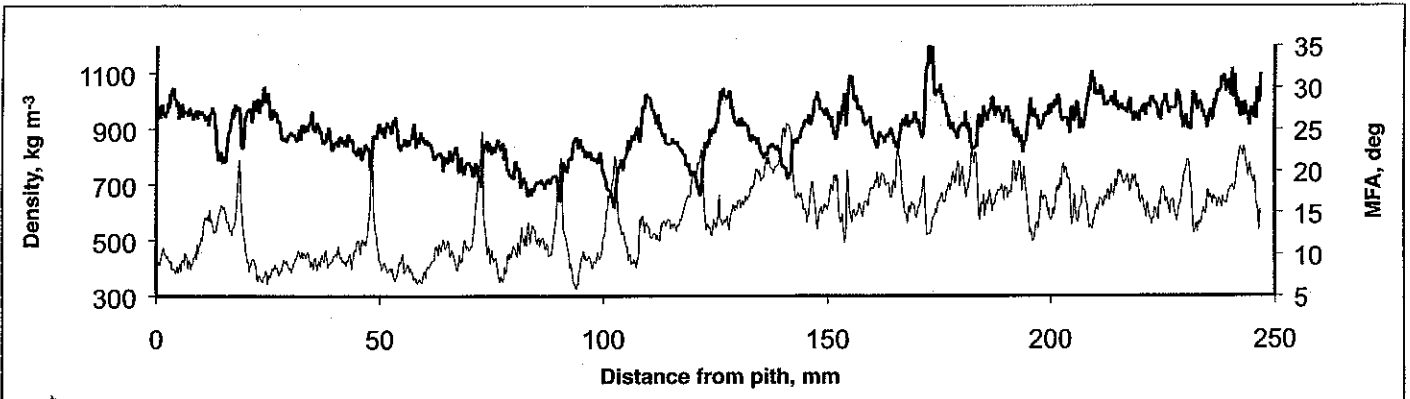


Fig. 15 High resolution MFA (thick line) and density (thin line) profiles for tree 68, 0.0 m level.

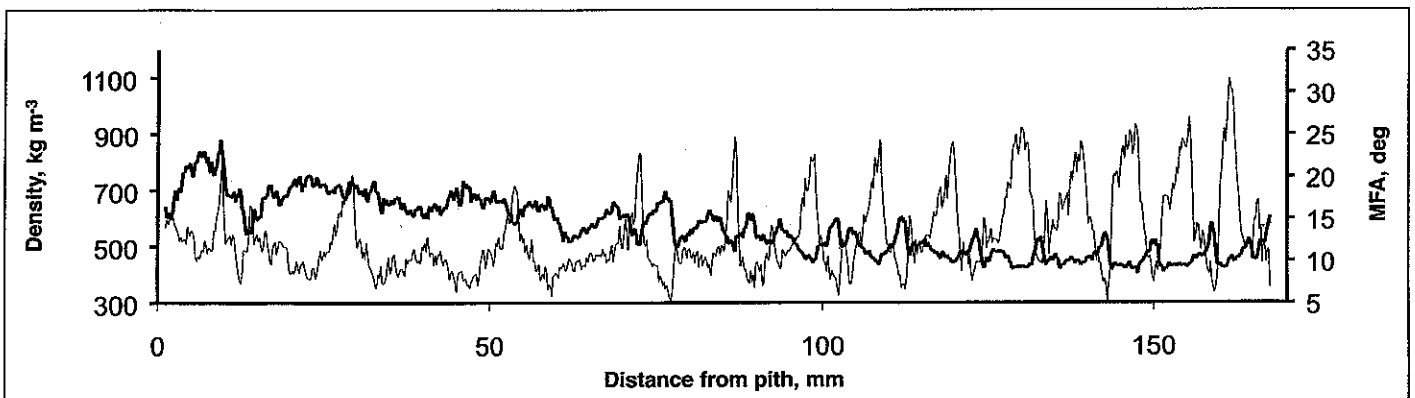


Fig. 16 High resolution MFA (thick line) and density (thin line) profiles for tree 43, 5.5 m level.

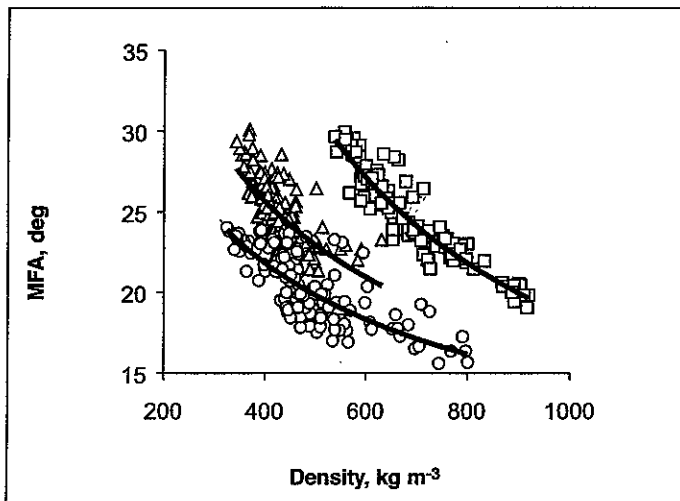


Fig. 17 Local relationships between MFA and density. All points were obtained from a single sample (tree 68, 0.0 m level). The three data subsets (from lower-left to upper-right) correspond to the sections 73-103 mm, 19-48 mm and 125-150 mm from the pith.

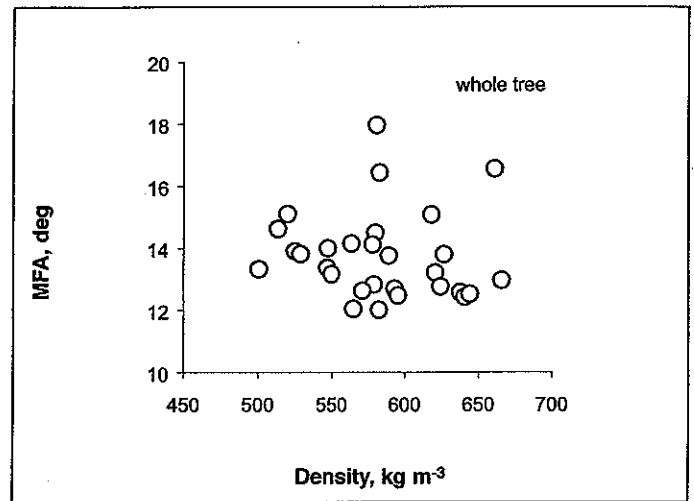


Fig. 18 Whole tree average MFA and density for the 29 *E. nitens* trees.

greater proportion of material in the S2 layer, which has a relatively low MFA. In addition, the transitional microfibrillar layers between S1 and S2, and between S2 and S3, become relatively less important as S2 (and the cell wall) thickens. Such effects would account qualitatively for the local inverse relationships observed between MFA and density, but the results presented in Figure 16 show that there must be mechanisms by which MFA and density (cell wall thickness) vary independently over longer time scales.

Density and MFA variation between trees.

We have demonstrated here and previously (2) that strong inverse correlations between MFA and density persist only for a few years. The results for average whole

tree properties are shown in Figure 18. As expected, there is no correlation between trees. It should therefore be possible to breed or select independently for MFA and density.

Variation of MFA and density with sampling height

On average, MFA decreased to a minimum at 30 to 50% of the tree height, then increased towards the top of the stem (Fig. 19). A more detailed examination of the MFA data shows that the position of minimum MFA within successive growth shells moves up the stem, remaining near a constant percentage of the shell height. A typical pattern is shown in Figure 20.

After a small drop near ground level, density increased with sample height, as shown in Figure 21. Closer examination

of the density data for individual growth shells shows even more complex behaviour than that found for MFA. Figure 22 indicates that density as a function of height within successive growth shells exhibits a minimum when the tree is young, levels out after about 10 years and may even exhibit a maximum in later years. The minimum (or maximum) appears to form near a constant percentage of shell height (30 to 50%).

Fibre orientation

Variations in fibre orientation adversely affect wood stiffness, strength and stability. The relative orientations of the fibres within the samples were measured using X-ray diffractometry (R. Evans, manuscript in preparation). Absolute fibre orientation within the trees could not be determined using

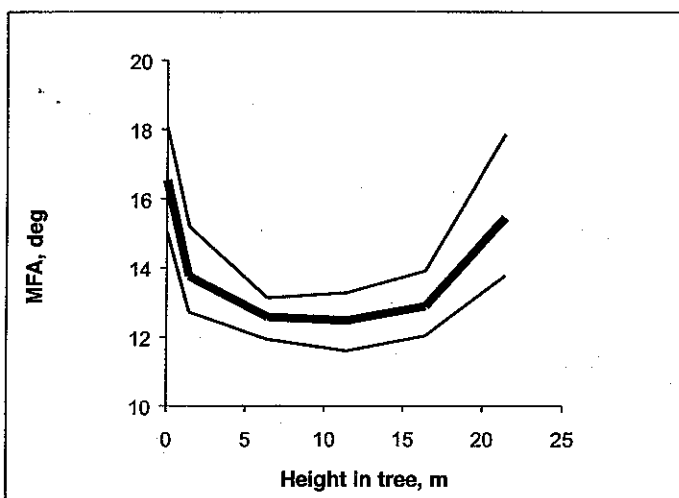


Fig. 19 Dependence of microfibril angle on sample height. The median line for the 29 trees is shown (thick line), together with upper and lower quartiles (thin lines).

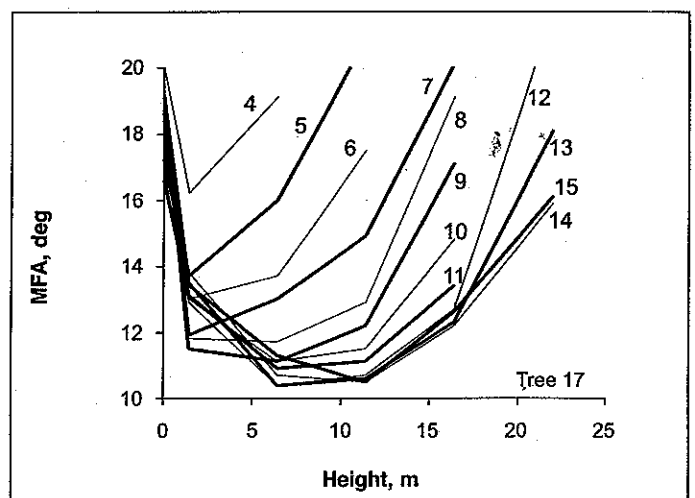


Fig. 20 Variation of MFA with height within individual growth shells. Tree age is indicated for each shell.

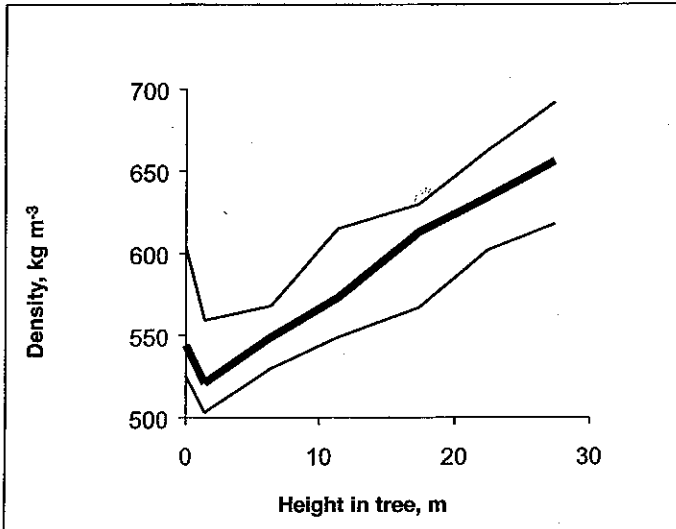


Fig. 21 Dependence of density on sample height. The median line for the 29 trees is shown (thick line), together with upper and lower quartiles (thin lines).

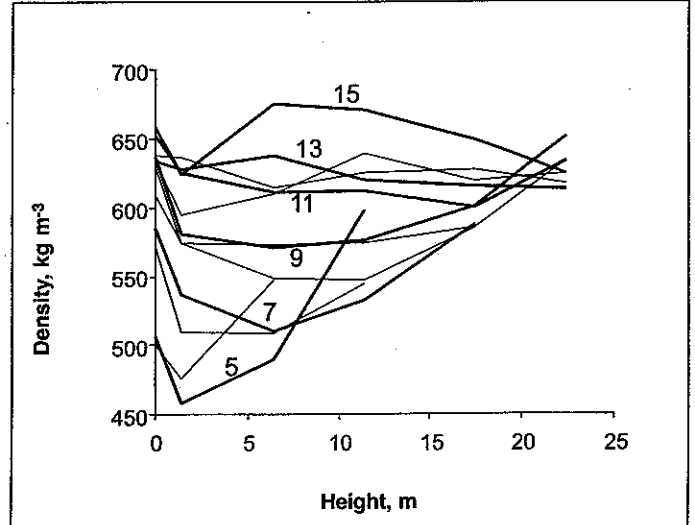


Fig. 22 Variation of density with height within individual growth shells. Tree age is indicated for alternate shells.

these samples because their original orientations relative to the stem were unknown. The results are summarised in Figure 23. For the experimental arrangement used on SilviScan-2, pitch is fibre tilt in the tangential direction (or spiral grain) and roll is radial tilt. Pitch and roll together describe fibre axis orientation in 3-dimensions. Yaw, which is not used in this report, describes the orientation of a fibre about its own axis.

Variability in fibre orientation was greatest at the base of the tree and decreased with increasing sampling height. Fibre pitch variation was consistently greater than roll variation. This result was expected, as the fibres in the cambium exist in an essentially 2-dimensional environment and have much greater orientational freedom in the tangential direction than in the radial direction.

CONCLUSIONS

Within these *E. nitens* trees, density and MFA exhibited consistent, complex patterns of variability. The most rapid changes in wood properties were observed near ground level. Variation in fibre orientation decreased with height within trees.

Breast height increment core properties were moderate to good predictors of whole tree MFA and density. However, prediction of whole tree properties was most efficient near the 5.5 m sampling height, which is only of interest in destructive sampling programs. Estimation of whole tree MFA and

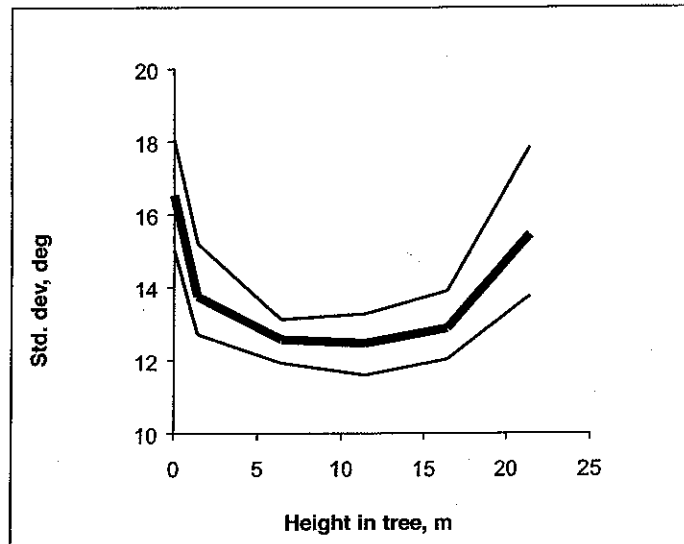


Fig. 23 Dependence of standard deviation of fibre axial orientation on sample height.

density from BH increment cores will require more samples to maintain precision.

Strong correlations between density and MFA were maintained only over short distances (up to a few annual growth rings).

Whole tree average MFA and density were uncorrelated, suggesting that these properties may be independently optimised in tree breeding programs.

ACKNOWLEDGEMENTS

The authors thank M. Lausberg of Carter Holt Harvey Forests for supplying the external dimensions and densities of the trees. The development of SilviScan-2 was funded by the Cooperative Research Centre for Hardwood Fibre and Paper

Science through the Australian Government's Cooperative Research Centre Programme.

REFERENCES

- (1) Kibblewhite, R. P., Riddell, M. J. C. and Shelbourne, C. J. A. - Kraft fibre and pulp properties of 29 trees of 15-year-old New Zealand-grown *Eucalyptus nitens*, *Appita J.* 51(2): 114 (1998).
- (2) Evans, R., Hughes, M. and Menz, D. - Microfibril angle variation by scanning X-ray diffractometry, *Appita J.* 52(5):363 (1999).
- (3) IAWA Bulletin n.s., Vol. 2 (2-3), 1981.
- (4) Chudnoff, M. - *Tropical timbers of the world*, Agric. Handbook 607, Washington DC, US Dept of Agriculture, 464pp. (1984).
- (5) Hiller, C. H. - Correlation of fibril angle with wall thickness of tracheids in summerwood of slash and loblolly pine, *Tappi J.* 47(2): 125 (1965).

Revised manuscript received for publication 15.5.00.

APPENDIX

Table A1
Summary of MFA analysis results for nominal sample heights and for whole trees.

Tree	Area-weighted MFA at nominal sample heights							Whole-tree mean MFA and percentiles					
	0	1.4	5.5	11	16.5	22	27.5	Mean	10%	25%	50%	75%	90%
3	17.6	15.7	14.6	12.7	14.1			12.6	10.1	10.4	11.7	14.1	16.0
9	20.0	20.0	14.6	14.1	15.5	16.9		14.2	10.6	11.9	13.9	15.4	18.3
11	16.4	13.0	12.1	12.0	13.9	18.7		12.6	9.5	9.9	11.4	14.1	17.8
13	17.1	14.4	13.1	12.7	12.4	14.1		11.9	9.7	10.2	11.3	13.3	14.8
16	17.0	15.5	12.8	12.0	12.9	15.5		11.9	9.7	10.0	11.1	13.1	15.3
17	20.9	16.2	15.2	15.2	15.4	18.6		13.9	10.7	11.4	13.0	15.9	18.7
35	18.6	16.5	14.6	15.2	14.6	15.0	14.7	14.1	11.6	12.1	13.3	15.3	17.7
37	17.5	15.5	15.3	13.4	14.3			12.8	10.1	10.8	12.3	13.9	16.2
42	21.8	18.8	18.2	17.6	19.3	19.7		16.3	11.7	12.7	15.6	19.1	23.1
43	18.6	16.6	14.6	14.3	14.2	15.0	16.8	13.7	11.0	11.9	13.1	15.2	17.2
49	19.3	14.9	13.7	14.2	16.7	19.0	16.7	13.1	9.6	10.4	11.8	15.3	18.2
50	17.2	16.5	16.3	16.0	15.8	19.0		15.1	12.1	13.2	14.6	16.7	18.8
55	19.2	16.5	13.3	13.7	13.9	20.6		13.9	11.0	11.3	12.7	15.9	18.4
57	18.9	17.1	15.2	14.7	15.6	18.8		14.5	11.0	12.2	14.2	16.1	18.7
60	20.1	16.1	13.0	13.6	13.8	18.4		13.3	10.7	11.3	12.6	14.8	16.9
61	15.8	14.3	13.0	13.1	13.2	12.9	16.5	12.4	10.4	10.9	12.0	13.5	14.7
63	16.4	14.8	13.7	13.0	14.1	15.6		12.4	10.1	10.7	11.4	13.8	15.7
64	17.9	15.1	14.2	14.9	15.5	16.0		13.7	11.1	12.0	13.2	15.1	16.9
68	24.7	20.4	20.9	15.5	15.8	19.4		18.0	12.8	15.0	17.1	21.2	23.6
73	20.1	22.0	14.2	15.2	14.0	16.3		14.9	10.6	11.9	14.6	17.3	19.7
76	18.8	15.0	12.8	11.7	13.2	13.3		12.3	9.7	10.4	11.5	13.9	15.9
77	17.7	15.8	15.3	14.7	16.1	19.7		13.7	10.0	11.2	13.2	15.2	18.3
81	18.1	14.1	12.9	11.5	15.2	16.1	17.0	12.7	10.1	10.9	11.9	13.7	16.6
84	17.9	17.1	15.8	16.7	16.9	21.2		14.1	10.9	11.3	12.6	15.7	20.7
85	22.4	19.9	17.9	15.9	15.3	17.6		16.4	11.6	13.2	16.1	19.5	22.0
90	16.8	14.6	14.6	14.1	16.1	19.5		13.3	10.1	10.6	12.1	15.1	17.7
91	16.4	13.9	13.4	12.7	13.8	18.3		12.5	10.2	10.9	12.1	13.3	15.7
93	19.3	17.2	14.6	15.1	14.3	15.9		13.0	9.3	10.2	12.2	14.9	18.0
98	18.1	14.6	13.9	12.6	12.8	16.7		12.9	10.2	11.2	12.2	14.0	16.4

Table A2
Summary of density analysis results for nominal sample heights and for whole trees.

Tree	Area-weighted density at nominal sample heights							Whole-tree mean density and percentiles						Basic density		
	0	1.4	5.5	11	16.5	22	27.5	Mean	10%	25%	50%	75%	90%	BH	Discs	Chips
3	531	513	542	599	669			595	424	484	579	681	798	430	473	479
9	588	492	558	591	618	644		583	398	461	551	678	820	433	466	494
11	603	582	596	622	647	667		638	467	529	612	723	866	466	508	533
13	525	503	549	578	582	634		571	397	453	544	661	795	400	456	475
16	542	503	557	567	640	639		584	413	474	569	686	781	427	457	480
17	517	494	503	538	587	579		549	374	423	515	646	783	396	436	454
35	586	535	536	569	566	605	615	579	425	479	564	667	765	460	467	466
37	516	520	534	562	618			582	401	453	550	681	833	434	467	488
42	543	511	556	587	626	634		584	422	476	563	664	784	428	466	490
43	623	529	536	572	557	598	618	590	420	474	559	685	827	430	471	464
49	584	566	573	621	629	638	656	624	471	525	599	704	821	456	502	506
50	544	477	487	519	542	625		520	383	433	496	586	697	390	424	411
55	548	519	475	486	505	557		526	375	424	502	620	715	388	417	406
57	521	475	478	520	524	558		515	361	404	477	597	744	404	425	437
60	500	440	481	513	514	579		501	348	396	471	570	708	376	409	390
61	607	580	597	633	631	673	702	642	480	537	624	734	830	479	521	492
63	610	535	560	603	608	625		599	432	479	555	687	852	432	465	484
64	510	489	528	519	541	625		530	379	427	498	608	738	385	415	435
68	574	537	568	573	595	671		587	415	481	584	682	761	431	468	484
73	542	536	565	679	640	683		622	443	504	604	718	835	435	484	492
76	610	663	585	599	621	658		647	457	516	619	757	898	479	491	494
77	600	602	555	624	644	667		631	461	514	603	721	856	475	492	498
81	661	559	581	615	613	648	692	625	451	515	609	715	830	496	505	497
84	535	521	533	549	567	689		565	408	460	530	638	790	427	451	431
85	636	621	589	635	691	647		666	478	535	643	791	890	525	530	452
90	498	505	539	557	589	626		549	388	441	521	625	760	392	435	462
91	544	528	530	566	614	599		573	413	465	540	641	805	435	463	456
93	509	483	514	536	596	567		554	374	419	505	642	849	382	444	456
98	673	635	617	621	630	793		669	473	530	651	798	895	532	533	556